

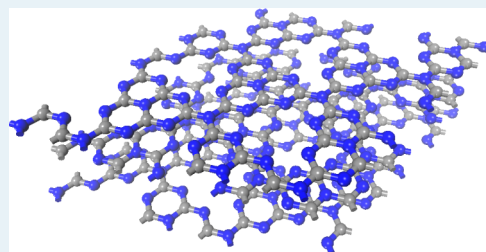
# Polymeric Graphitic Carbon Nitride for Heterogeneous Photocatalysis

Xinchen Wang, Siegfried Blechert,<sup>†</sup> and Markus Antonietti\*

International Joint Laboratory between Max-Planck Institute of Colloids and Interfaces, Department of Colloid Chemistry, Research Campus Golm, 14424 Postdam, Germany, and Research Institute of Photocatalysis, State Key Laboratory Breeding Base of Photocatalysis, Fuzhou University, Fuzhou 350002, China

**ABSTRACT:** Polymeric graphitic carbon nitride (for simplicity,  $g\text{-C}_3\text{N}_4$ ) is a layered material similar to graphene, being composed of only C, N, and some impurity H. Contrary to graphenes,  $g\text{-C}_3\text{N}_4$  is a medium band gap semiconductor and an effective photocatalyst for a broad variety of reactions, and it possesses a high thermal and chemical stability. In this Perspective, we describe the polycondensation of this structure, how to modify band positions and band gap by doping and copolymerization, and how to texture the organic solid to make it an effective photocatalyst. We then describe the photochemical splitting of water and some mild and selective photooxidation reactions catalyzed by  $g\text{-C}_3\text{N}_4$ .

**KEYWORDS:** carbon nitride, photocatalysis, selective oxidation, heterogeneous organocatalysis



## 1. INTRODUCTION

Photocatalysis enables one to use light to drive catalytic reactions. The extra energy brought in by the photon can be employed to accelerate an otherwise kinetically hindered reaction; however, it can also be used to run a reaction that is otherwise energetically unfavorable. If the photocatalyst is well chosen, the use of a photoactive center can in addition bring high chemo- and regioselectivity. A last point is that photocatalysis can be inherently “green”, that is, using photons and possibly water as a solvent is a per se sustainable but also very effective approach. All these advantages have stimulated the search for new photocatalysts.

In recent years, carbon nitride has turned out to be a fascinating choice for a photocatalyst; however, this substance is not new at all. A polymeric derivative has already been made by Berzelius and named by Liebig in 1834 as “melon” and is to be regarded as one of the oldest synthetic polymers.<sup>1</sup> A more detailed discussion of actual synthesis routes will be presented below, but it is interesting to recognize that this polymeric semiconductor is composed of mainly carbon and nitrogen, for which organic chemistry provides reactions and tools to modify its reactivity without having to change the overall composition too much. Indeed, reports on approaching the synthesis of different modifications and the elucidation of the composition and structure of carbon nitride materials abound in the literature.<sup>2–15</sup> Its potential applications in energy conversion,<sup>16,17</sup> hydrogen<sup>18–20</sup> and carbon dioxide storage,<sup>21</sup> purification of contaminated water,<sup>22</sup> in solar cells,<sup>23–25</sup> and as humidity and gas sensors,<sup>26,27</sup> etc. have also been reported.

Graphitic carbon nitride,  $g\text{-C}_3\text{N}_4$ , is the most stable allotrope of carbon nitride and has been the object of intense research in recent years.<sup>28–34</sup> The framework topology previously identified in  $g\text{-C}_3\text{N}_4$  is, in fact, presumably a defective, N-bridged “poly(tri-

$s$ -triazine)”. Since the  $s$ -triazine ring ( $\text{C}_3\text{N}_3$ ) is aromatic, it is nearby that a conjugated, two-dimensional polymer of  $s$ -triazine tends to form a  $\pi$ -conjugated plane such as that of graphite, and this has been proven by wide-angle X-ray diffraction (XRD) patterns, SEM, and TEM observations.<sup>35–38</sup> The tri- $s$ -triazine ring structure and the high condensation makes the polymer possess high stability with respect to thermal (up to 600 °C in air) and chemical attacks (e.g., acid, base, and organic solvents) and provides it with an appealing electronic structure, being a medium band gap, indirect semiconductor.<sup>28,39,40</sup> Interestingly, many organic and inorganic compounds or metals could bind to the matrix and allow tuning the reactivity of  $g\text{-C}_3\text{N}_4$ , if desired. Such protocols are already widely used to control the performance of carbon nitride. Examples include protonation<sup>43</sup> and boron,<sup>41</sup> fluorine,<sup>38</sup> and sulfur doping.<sup>44,45</sup> The introducing of such functional atoms or groups into the matrix or surface of the carbon nitride greatly improved its performance.

It is the purpose of the present Perspective to review for nonexperts what is known about the chemistry of carbon nitride and how to improve its composition, structure, and texture for catalytic applications. Finally, we will describe the fascinating world of photocatalysis with carbon nitride describing both photon-induced water splitting (artificial photosynthesis) and novel smooth photooxidation and coupling schemes of organic molecules.

## 2. CARBON NITRIDE THROUGH THE CENTURIES

As already mentioned, the history of carbon nitride and its precursors started in the very early days of Berzelius and Liebig in

Received: April 11, 2012

Revised: June 14, 2012

Published: July 9, 2012

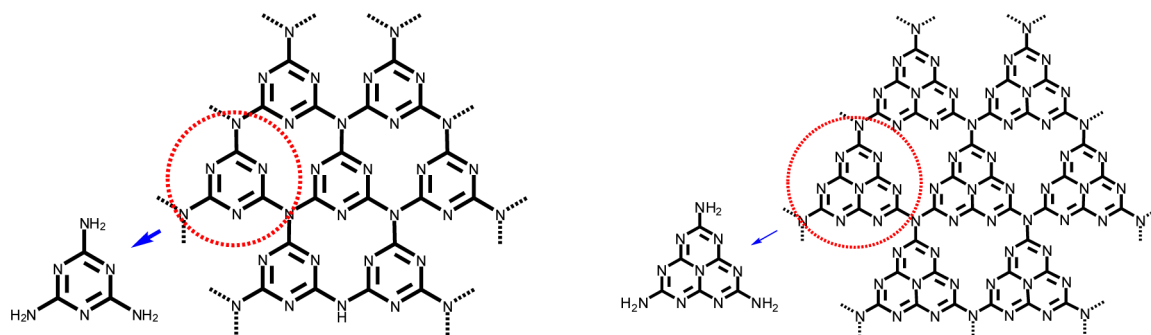


**Figure 1.** *s*-Triazine (left) and tri-*s*-triazine as tectons of  $g\text{-C}_3\text{N}_4$ .

1834.<sup>1</sup> Closer insights into the structure of these compounds were described by Franklin as early as 1922. He introduced the concept of “carbonic nitride” ( $\text{C}_3\text{N}_4$ ) and suggested that  $\text{C}_3\text{N}_4$  might be obtained as the final deammonation product of the series of ammono carbonic acids.<sup>47</sup> Pauling and Sturdivant first suggested a coplanar tri-*s*-triazine unit as the basic structural motif of these polymeric derivatives in 1937.<sup>48</sup> Later, Redemann and Lucas indicated that there is a formal resemblance between melon and graphite. They deduced that the Franklin’s carbon nitride can be described as an oligomeric condensation product of 2,5,8-triamino-tris-*s*-triazine; that is,  $\text{C}_{126}\text{H}_{21}\text{N}_{175}$ .<sup>49</sup> On the basis of these findings, it was stated that probably not one single structure should be assigned to melon because it is more likely a mixture of polymers of different sizes and architectures.

The above melon-based carbon nitrides have been forgotten for a long time as unconfirmed species. One reason why their structures remained unclear in detail until today is their chemical inertness and their insolubility in practically all solvents. In the 1990s, more than 150 years later, interest in carbon nitrides was restimulated by the theoretical prediction that the dense  $sp^3$ -bonded  $\text{C}_3\text{N}_4$  phase ( $\beta\text{-C}_3\text{N}_4$ ) could have extremely high bulk modulus and hardness values, comparable with or exceeding that of diamond.<sup>50–54</sup> However, it turned out to be very difficult to prepare single-phase  $sp^3$ -hybridized carbon nitride phases because of its low thermodynamic stability.<sup>55,56</sup> Further theoretical work indicated  $g\text{-C}_3\text{N}_4$  to be the most stable allotrope at ambient conditions.<sup>53,57–59</sup> The synthesis and characterization of  $g\text{-C}_3\text{N}_4$  is a challenging task by itself, and until today, a large number of different experimental attempts have been made.<sup>4,10,60–67</sup> Reviews on this structural part of carbon nitride were recently given by Kroke,<sup>16</sup> Antonietti,<sup>28</sup> Blinov,<sup>46</sup> and Matsumoto et al.<sup>68</sup>

Because of the lack of experimental data, there is a prevailing discussion about the actual existence of a graphitic material with idealized composition  $\text{C}_3\text{N}_4$  and possible structure models for  $g\text{-C}_3\text{N}_4$ . Inspired by the structure of graphite, triazine ( $\text{C}_3\text{N}_3$ ) had been put forward as elementary building blocks of  $g\text{-C}_3\text{N}_4$  (Figure 1),<sup>16,31,53,57–59,69–84</sup> however, another possible block, tri-*s*-triazine (heptazine) rings, which are structurally related to the melon,<sup>1,47,85–88</sup> were shown to be energetically favored with respect to the triazine-based modification.<sup>82,89</sup> These tri-*s*-triazine rings are cross-linked by trigonal N atoms (Figure 1), and most recent works show that, indeed, the pyrolysis of cyanamide, dicyandiamide, or melamine yields a melon polymer built up from melem units,<sup>32,36,60,61,63,71,82,89–92</sup> confirming that this tecton is the most stable local connection pattern.

Until now, the condensation pathways of cyanamide to dicyandiamide and later to melamine were seen as good synthetic strategies to generate slightly defective, polymeric species. It

must be noted that this approach is simple and convenient and allows mass production of carbon nitrides with high catalytic activity for prices in the range of a few euros per kilogram.

From the perspective of the fundamental understanding of materials structures, it is still challenging to synthesize more perfect, crystalline carbon nitride. The bulk synthesis routes based on these C/N/H-containing compounds—despite numerous attempts—have not yielded the desired, ideally condensed, crystalline  $\text{C}_3\text{N}_4$  phase. This is widely acknowledged as being a predominantly kinetic problem,<sup>28</sup> and medium to poor crystallinity and a high degree of disorder of the as synthesized material are typical for all active products.

From the viewpoint of applied photocatalysis, we can state that until now, the by far more active materials have all been slightly disordered; that is, stacking defects, grain boundaries, surface termination, or even structural defects are an inherent, if not a mandatory part of a catalyst, whereas crystalline perfection “only” contributes to the bulk properties, such as the graphitic structure, high thermal and chemical stability, semiconductor electronic structure, etc.<sup>28,46</sup> In addition, understanding carbon nitride as a polydisperse polymer enables one to apply diverse synthetic tools, such as copolymerization with similar tectons, curvature and nanostructure design, or templating to generate a high specific surface area.

The potential applications of  $g\text{-C}_3\text{N}_4$  as an organic semiconductor in the catalysis fields have been seriously neglected until the discovery of its application as metal-free heterogeneous catalyst in 2006.<sup>93,94</sup> Since then, the application of carbon nitride or its modifications in sustainable chemistry is literally exploding, with only little chance to catch all the current activities of the field in a balanced fashion.

### 3. USEFUL PROPERTIES OF CARBON NITRIDE

Thermal analysis (TGA) on  $g\text{-C}_3\text{N}_4$  reveals that this material is significantly robust and nonvolatile up to 600 °C, even under air. A strong endothermic peak appears at 630 °C, paralleled by consecutive complete weight loss, indicating thermal decomposition and complete vaporization of the fragments. This thermal stability is, however, one of the highest for an organic material and, for instance, higher than those of all high-temperature polymers, such as aromatic polyamides and -imides. Note that the thermal stability of carbon nitride somewhat differs between different preparation methods,<sup>36,42,66,95,96</sup> which may be due to different degree condensation and different packing motifs.

Similar to that of graphite, the stacking with optimized van der Waals interactions between the single layers of carbon nitride makes it insoluble in most solvents. No detectable solubility or reactivity of carbon nitride in conventional solvents, including

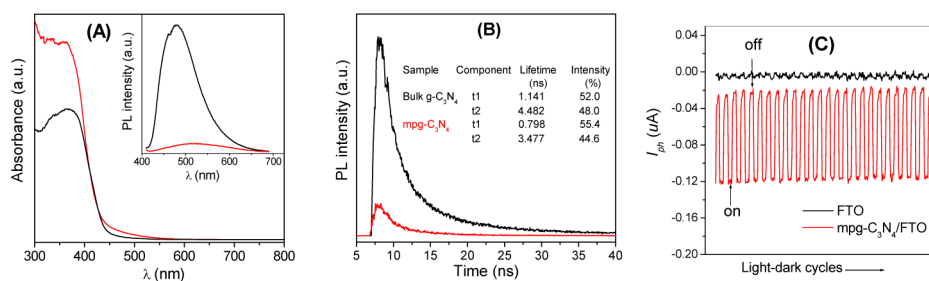


**Figure 2.** (A) Diffuse reflectance absorption spectrum and photoluminescence (PL) spectrum (inset) under 420 nm excitation and (B) time-resolved PL spectrum monitored at 525 nm under 420 nm excitation at 298 K for bulk g-C<sub>3</sub>N<sub>4</sub> (black) and mpg-C<sub>3</sub>N<sub>4</sub> (red). (C) Periodic on/off photocurrent  $I_{ph}$  response of mpg-C<sub>3</sub>N<sub>4</sub> electrode in 0.5 M Na<sub>2</sub>SO<sub>4</sub> under zero bias in a standard two-electrode photoelectrochemical cell. Reproduced with permission from ref 101; copyright 2009, American Chemical Society.

water, alcohols, DMF, THF, diethyl ether, toluene, et al., has been observed.<sup>95</sup> There are two exceptions: treating g-C<sub>3</sub>N<sub>4</sub> in molten alkali hydroxides results in a hydrolysis of the structure. Treatment in concentrated acids, on the other hand, leads to colloidal, presumably sheetlike dissolution,<sup>43</sup> which, however, is fully reversible.

The optical properties of the carbon nitride can be accessed by most simple experiments as UV-vis absorption and photoluminescence. As revealed by the theoretical calculations, the polymeric carbon nitride is a typical semiconductor.<sup>97</sup> Indeed, conventional disordered carbon nitride shows the typical absorption pattern of an organic semiconductor with a very strong, stepwise gap adsorption at about 420 nm (Figure 2A). This is consistent with its pale yellow color. The preparation method including the choice of precursor or condensation temperature slightly affects the absorption edge of carbon nitride, which again may be due to the different local structure, packing, and defects formed during the preparation or modification processes.<sup>40,42</sup> For example, different modifications of carbon nitride may lead to the blue shift (such as protonation<sup>43</sup> or sulfur doping<sup>44</sup>) or red shift (boron and fluorine doping<sup>38</sup> and copolymerization with barbituric acid<sup>99</sup>) of the adsorption edge. This absorption spectrum determines the range of used photons in the photocatalysis experiment.

Several photoluminescent species have been reported, and some of them exhibit emission in the blue region. It seems that the photoluminescence spectrum sensitively depends on the degree of condensation and the packing between the layers.<sup>28,61,66,98,100</sup> Generally, ordinary polymeric carbon nitride exhibits strong blue photoluminescence at room temperature. The luminescence covers a broad range (430–550 nm) and peaks at ~470 nm. The lifetime of this fluorescence is in the range of 1–5 ns. (Figure 2B) It must also be mentioned that the fluorescence can be highly quenched when introducing a high specific surface area; that is, the photogenerated charges are then stabilized at the interfaces. This is important for their use in photochemistry.

The suitable electronic band structure makes the carbon nitride a promising candidate for solar energy converting systems, such as photoelectrochemical cells (Figure 2C).<sup>24</sup> Indeed, photocurrent was observed even in the case of bulk g-C<sub>3</sub>N<sub>4</sub> under the illumination of visible light ( $\lambda > 420$ ).<sup>24,29,99</sup> The high chemical and thermal stability of the carbon nitride allows operation of a photoelectrochemical cell under oxygen atmosphere, which is exceptional. In addition, the electronic band structures of g-C<sub>3</sub>N<sub>4</sub> could be well tuned by modification of nanomorphology or doping, which makes the improvement of photocurrent possible. For example, mesoporous carbon nitride

(mpg-C<sub>3</sub>N<sub>4</sub>) can, in principle, enhance the light-harvesting ability due to its large surface and multiple scattering effects and therefore showed increased photocurrent.<sup>101</sup> Other modifications, including doping and protonation, can also increase the photocurrent.<sup>24,29,99</sup> Figure 3 depicts the positions of the valence

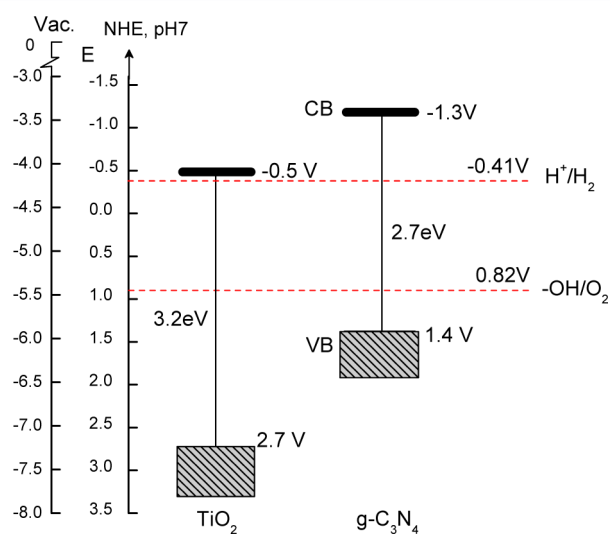


**Figure 3.** Electronic band structure of g-C<sub>3</sub>N<sub>4</sub>, compared with the well-known golden inorganic photocatalyst, titanium dioxide (TiO<sub>2</sub>). Reproduced with permission from ref 133; copyright 2012, Royal Society of Chemistry.

band (VB) and conduction band (CB) of mpg-C<sub>3</sub>N<sub>4</sub>, in comparison with the golden photocatalysis standard TiO<sub>2</sub>. It is seen that in mpg-C<sub>3</sub>N<sub>4</sub>, the water oxidation and reduction potentials are much better engulfed, which means that mpg-C<sub>3</sub>N<sub>4</sub> is, in principle, able to run both the oxygen and hydrogen evolution from water.

#### 4. CHEMICAL VARIATION OF CARBON NITRIDE

The carbon nitride materials collected directly after self-condensation of organic precursors are macropowders with a very small surface area, normally below 10 m<sup>2</sup>/g. For practical applications of the materials in fields such as (photo)catalysis, the introduction of controlled porosity at the nanoscale in the bulk carbon nitride is mandatory to enhance its function. Starting from a liquid precursor and making a material by condensation, however, enables a multitude of processing steps, including printing, stamping, spinning, film casting, molding, templating, or extrusion. For the creation of high specific surface area, nanocasting is advisable.<sup>102</sup>

First, mesoporous  $g\text{-C}_3\text{N}_4$  (mpg- $\text{C}_3\text{N}_4$ ) was obtained by nanocasting/replication of mesoporous silica matrixes, well-known from the generation of the corresponding carbon nanostructures.<sup>35,103,104</sup> In a typical synthetic procedure, the silica template and organic precursor (for example, cyanamide) were first mixed in aqueous solutions. After removing water, the resulting composite was subsequently heated for 4 h at 550 °C, ensuring the condensation of the precursor into polymeric  $\text{C}_3\text{N}_4$ . Removing the silica template with an aqueous  $\text{NH}_4\text{HF}_2$  solution yielded the carbon nitride replica as a yellow powder. By utilizing this “hard template” method, the morphological properties of carbon nitride can be controlled to a certain extent, featuring surface areas between 86 and 439  $\text{m}^2 \text{g}^{-1}$ , depending on the weight fraction of the silica template.<sup>28,93</sup> Subsequently, ordered mesopore carbon nitrides with different mesostructures have also been synthesized using SBA-15 as a hard template.<sup>105,106</sup>

In addition to that, the use of “soft templates” for making mesoporous carbon nitrides is of growing interest.<sup>107–109</sup> Owing to thermodynamic and physicochemical reasons, preparing porous materials using soft templates is sometimes still a challenge.<sup>103,110–112</sup> Boron- and fluorine-doped polymeric carbon nitride solid has been synthesized by using butylmethylimidazolium- $\text{BF}_4$  as a soft template.<sup>29</sup> These doped carbon nitride materials exhibited outstanding mesoporous textural properties, with pore volumes and sizes equal to materials prepared via the mentioned hard template routes. For example, a sample CNBF-0.5 exhibited a specific Brunauer–Emmett–Teller (BET) surface area of 444  $\text{m}^2 \text{g}^{-1}$  and a total pore volume of 0.32  $\text{m}^3 \text{g}^{-1}$ , whereas micropores are essentially absent in carbon nitrides.

Moving to chemical modification of catalysts in general, doping with ternary elements is a standard approach, and this is also true for carbon nitride. The effects of doping carbon nitride with boron,<sup>41</sup> fluorine,<sup>38</sup> sulfur,<sup>44</sup> and other elements are well documented. Sulfur doping could, for instance, be obtained by treating the fresh  $g\text{-C}_3\text{N}_4$  at 450 °C in gaseous  $\text{H}_2\text{S}$  atmosphere.<sup>44</sup> For P-doping, the ionic liquid 1-butyl-3-methylimidazolium hexafluorophosphate ( $\text{BmimPF}_6$ ), was selected as a mild phosphorus. This phosphorus-doped carbon nitride provided not only a much better electric conductivity of up to 4 orders of magnitude but also an improvement in photocurrent generation by a factor of up to 5.<sup>113</sup>

The application of aminoborane as a comonomer allowed replacement of the carbon atoms in  $g\text{-C}_3\text{N}_4$  with boron (Figure 4). Because BN also follows a strictly planar, graphitic morphology, the overall structure of  $g\text{-C}_3\text{N}_4$  is very well kept, whereas the boron sites on the surface might act as strong Lewis acid sites, thus complementing the basic nitrogen sites to enable bifunctional catalysis.

Structural details of the incorporation of boron into the C/N matrix were obtained with  $^{11}\text{B}$  solid-state MAS NMR and XPS experiments. The  $^{11}\text{B}$  NMR spectrum nicely reveals two peaks indicating two different positions in the framework structure, presumably as a corner boron and bay boron (Figure 4b).

Another modification method includes the copolymerization of the nitrogen precursor (for example, dicyandiamide) with other organic additives, such as barbituric acid,<sup>99</sup> and organic comonomers containing cyano or amino groups or both (as exemplified in Figure 5a). Contrary to inorganic modification schemes, the modified carbon nitride based on organic copolymerization shows a remarkable red shift of optical absorption from 470 to 750 nm with increasing comonomer

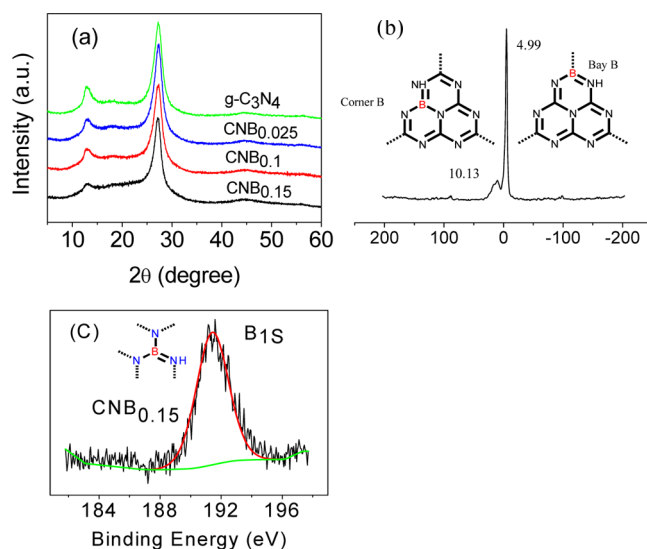


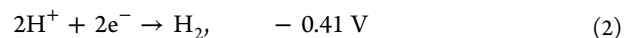
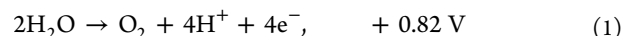
**Figure 4.** (a) XRD patterns of the B-doped and pristine  $g\text{-C}_3\text{N}_4$ , (b)  $^{11}\text{B}$  solid-state MAS NMR spectra of  $\text{CNB}_{0.15}$ . Inset: the building unit of  $\text{C}_3\text{N}_4$  with B doping at the bay-carbon site (right) and at the corner-carbon site (left), (c) XPS spectra of  $\text{CNB}_{0.15}$ . Reproduced with permission from ref 114; copyright 2010, Royal Society of Chemistry.

content, which would allow photochemical application of wavelengths in which the solar photon flux is maximal (Figure 5).

## 5. CARBON NITRIDE AS A PHOTOCATALYST

**5.1. Photochemical Water Splitting.** In the following section, we will summarize some of the recent, most remarkable examples of using  $g\text{-C}_3\text{N}_4$  in photocatalysis. Direct water splitting using a photocatalyst with visible light is the silver bullet to produce hydrogen fuel, thus converting sunlight into storable and transportable energy in chemical bonds.<sup>115,116</sup> To date, studies on heterogeneous photocatalysis have mainly focused on the development of materials with a sufficiently small band gap and suitable band positions for overall water splitting, accompanied by adequate stability for practical applications.<sup>117</sup> Most of these semiconductor materials were solely inorganic and metal-based, comprising metal oxides, nitrides, sulfides, phosphides, and their mixed solid solutions.<sup>118</sup> In nature, metal-based complexes can be found in enzymes as active centers for photocatalyzing the decomposition of water, but the overall system is rather a biopolymer structure, which is rather different from an ordinary, technical heterogeneous catalyst.

Owing to its structural and electronic properties,  $g\text{-C}_3\text{N}_4$  contains all the prerequisites required for a heterogeneous photocatalyst; it has the correct electronic structure with an appropriate band gap of 2.7 eV, corresponding to an optical wavelength of 460 nm. This band gap is sufficiently large to overcome the endothermic character of the water-splitting reaction. To produce hydrogen from water, the endothermic character of the water-splitting reaction has to be overcome. The theoretically required energy to produce hydrogen from water is calculated in eqs 1 and 2.



Equations 1 and 2 agree with the redox potentials converted to NHE reference at pH 7. The necessary energy of the catalyst to overcome the band gap for hydrogen production therefore

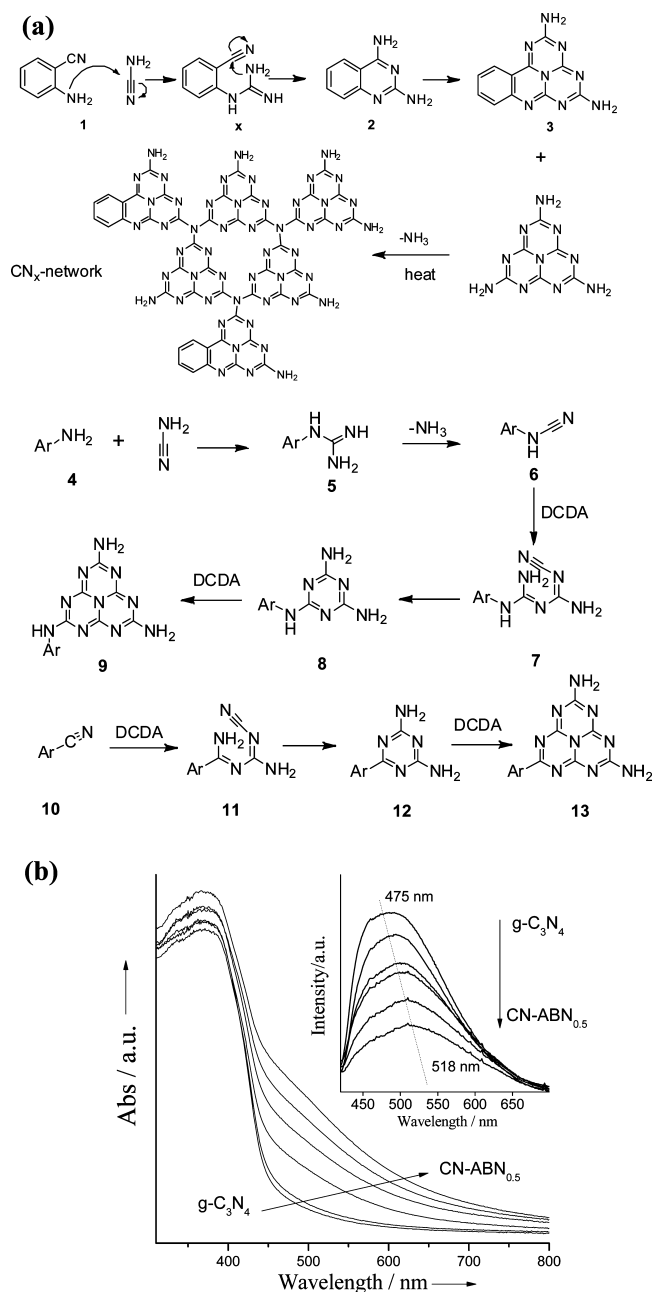


**Figure 5.** (a) The copolymerization of dicyandiamide/cyanamide with 2-aminobenzonitrile (ABN), aniline, and benzonitrile. (The linkers (3,9,13) can be integrated into the classic condensation scheme of  $g\text{-C}_3\text{N}_4$ .) (b) Optical absorption and photoluminescence (PL) spectrum (inset) of 2-aminobenzonitrile-functionalized  $g\text{-C}_3\text{N}_4$  ( $\text{CN-ABN}_x$ , where  $x$  refers to the amount of ABN), together with pristine  $g\text{-C}_3\text{N}_4$  reference. Reproduced with permission from ref 134; copyright 2012, Wiley-VCH.

requires 4 photons with at least 1.23 V. Because some of the intermediates of the 4-electron transfer are higher in energy, a certain “inherent overpotential” has to be considered, which makes photons exceeding about 1.8 eV energy (or higher) practically suitable for this reaction. This corresponds to a wavelength of light of 690 nm and shorter.

Consequently, to run photosplitting of water with a photocatalyst, the band gap of the structure has to be larger than this value. Because light absorption is accompanied by a number of instantaneous molecular relaxations, as a rule of thumb, the

fluorescence wavelength can be taken as a measure for the energy available for the reaction.

In addition, however, the band gap has to be placed in a way that the photogenerated hole has enough oxidation strength to oxidize water to  $\text{O}_2$ , and the photogenerated electron has to be reductive enough to reduce water to  $\text{H}_2$ ; that is, the HOMO–LUMO band positions have to engulf the redox potential of water. This is graphically illustrated in Figure 6 with the calculated band positions of carbon nitride,<sup>24</sup> which is, indeed, able to run both half reactions independently.

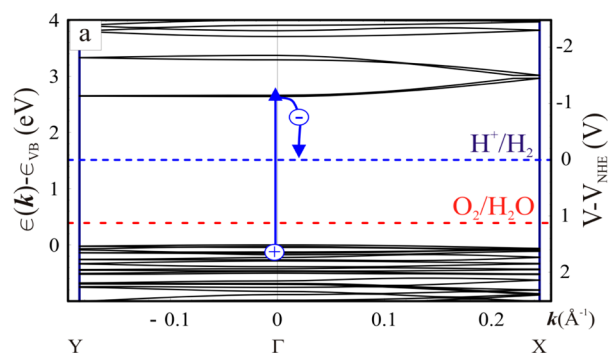


**Figure 6.** Density functional theory band structure for polymeric melon calculated along the chain ( $\Gamma\text{-}\chi$  direction) and perpendicular to the chain ( $\gamma\text{-}\Gamma$  direction). The position of the reduction level for  $\text{H}^+$  to  $\text{H}_2$  is indicated by the dashed blue line, and the oxidation potential of  $\text{H}_2\text{O}$  to  $\text{O}_2$  is indicated by the red dashed line just above the valence band. Reprint with permission from ref 28; copyright 2008, Royal Society of Chemistry.

This type of engulfing is a rare case in organic semiconductors and implies, for instance, that the photocatalyst is stable against oxygen and water, which is rare again (the other case being photocorrosion). The typical reaction cascades are schematically illustrated in Figure 7.

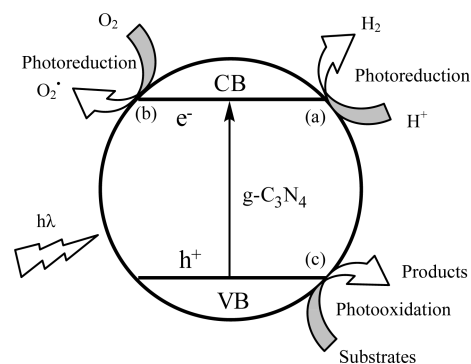


**Figure 7.** Strategies to realize visible light induced photocatalysis: (a) hydrogen evolution from water, (b) photochemical activation of  $\text{O}_2$ , and (c) photocatalytic oxidation or degradation of organic substrates.

Moreover,  $g\text{-C}_3\text{N}_4$  exhibits an appropriate microstructure, with surface termination with defects and nitrogen atoms for electron localization or for anchoring the active sites. In a recent contribution, this material was, indeed, used as an efficient and inexpensive photocatalyst for water splitting under visible light in the presence of external redox agents.<sup>40,119</sup>

A  $g\text{-C}_3\text{N}_4$  catalyst exhibits activities for water reduction into  $\text{H}_2$  or water oxidation into  $\text{O}_2$  in the presence of a proper sacrificial electron donor or acceptor, even in the absence of noble metal

catalysts (Figure 8).<sup>40,119</sup> Until to now, however, efficient and stable H<sub>2</sub> evolution could be achieved only by modification off

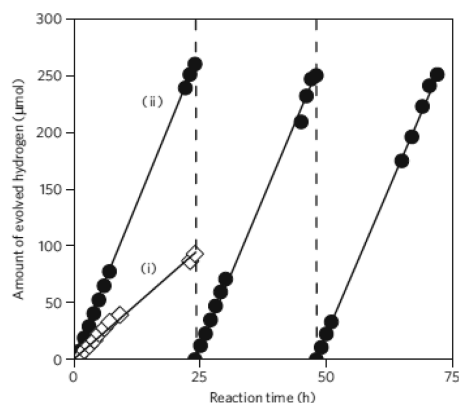


**Figure 8.** Stable hydrogen evolution from water by g-C<sub>3</sub>N<sub>4</sub>. A typical time course of H<sub>2</sub> production from water containing 10 vol % triethanolamine as an electron donor under visible light (of wavelength longer than 420 nm) by (i) unmodified g-C<sub>3</sub>N<sub>4</sub> and (ii) 3.0 wt % Pt-deposited g-C<sub>3</sub>N<sub>4</sub> photocatalyst. The reaction was continued for 72 h, with evacuation every 24 h (dashed line).

the g-C<sub>3</sub>N<sub>4</sub> with a small amount of cocatalyst, such as Pt. This is presumably due to kinetic effects because splitting of the Pt–H bond is much less kinetically hindered than the homolytic splitting of a covalent N–H bond.

The estimated quantum efficiency of the g-C<sub>3</sub>N<sub>4</sub> in these primary experiments was still rather low (~0.1% with irradiation of 420–460 nm), even with the help of Pt. This can be attributed to charge recombination by inner grain boundaries and a nanostructure not optimized for the lifetime of the photoexcited charge pairs.

A high dispersion of cocatalysts on the g-C<sub>3</sub>N<sub>4</sub> surface is favorable.<sup>119</sup> For example, bis(1,5-cyclooctadiene)platinum complex (Pt(cod)<sub>2</sub>) was found to be a better precursor than H<sub>2</sub>PtCl<sub>6</sub> for better access of Pt(cod)<sub>2</sub> to the g-C<sub>3</sub>N<sub>4</sub> surface, which caused a better dispersion of Pt nanoparticles on g-C<sub>3</sub>N<sub>4</sub>. Modification with RuO<sub>2</sub> can improve the stability against the self-decomposition of g-C<sub>3</sub>N<sub>4</sub> and improves the O<sub>2</sub> evolution activity.<sup>119</sup> Au/g-C<sub>3</sub>N<sub>4</sub> prepared by a deposition–precipitation method also shows improved photocatalytic activity due to the formation of tight Au-semiconductor heterojunctions effectively promoting the transfer of charge from light-excited g-C<sub>3</sub>N<sub>4</sub>.<sup>120</sup> Recently, Ye and co-workers reported that carbon nitride polymer sensitized with N-doped tantalum acid showed a high photocatalytic activity and good stability for hydrogen evolution from an aqueous methanol solution under visible light (>410) irradiation, and up to 4.8% of the apparent quantum yield was achieved at 420 nm.<sup>121</sup>

One can expect that the modification of textural structure of g-C<sub>3</sub>N<sub>4</sub> can, in principle, enhance the light-harvesting ability of the materials as a result of a larger surface and optimized charge separation. Indeed, the efficiency of hydrogen production from the photochemical reduction of water could be improved by 8.3 times via introducing mesoporosity into g-C<sub>3</sub>N<sub>4</sub> (Table 2).<sup>101</sup>

An alternative approach to enhance photoelectric performance of carbon nitride polymers is improving the crystallinity, which can, in principle, promote the kinetics of charge diffusion in both the bulk and on the surface. Conventional photoactive g-C<sub>3</sub>N<sub>4</sub> is a polymeric, slightly distorted solid, and highly condensed g-C<sub>3</sub>N<sub>4</sub> is believed to have higher carrier mobility and lower

HOMO levels because of fewer defects in the network, which promises to improve the oxidation power. Translating the bulk polycondensation into nanodimensional volume is considered an effective approach to address the kinetic problems by lowering the topological complexity of the confined polymer, which in addition offers a direct tool toward nanofabrication of carbon nitride heterostructures with improved charge separation and collection. A recent study showed that confined thermal condensation of cyanamide inside channels of porous anodic alumina oxide (AAO) membrane templates can efficiently increase the crystallinity, extending the domain size and lowering the HOMO position of g-C<sub>3</sub>N<sub>4</sub>-based materials (Figure 9). The

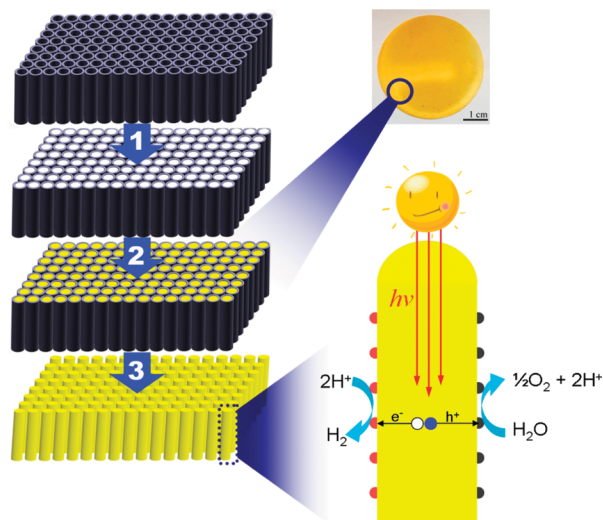


**Figure 9.** AAO-templating approaches toward CNR via three steps: (1) filling the AAO template (gray) with monomer cyanamide (white), (2) heating the filled templates at 600 °C under N<sub>2</sub> flow for 4 h, and (3) etching the template to release CNR (yellow). Top right: photograph of CNR in AAO before removing the template. Bottom right: proposed reaction mechanism of water oxidation and reduction. Reprinted from ref 122, copyright 2011, American Chemical Society.

as-obtained carbon nitride nanorods (CNRs) offer a higher oxidation power, as exemplified by the O<sub>2</sub> revolution from water. Although mesoporous g-C<sub>3</sub>N<sub>4</sub> (surface area, 190 m<sup>2</sup>/g; O<sub>2</sub> evolution rate, 3.8 µmol/h) and the bulk phase (3.9 µmol/h) showed comparable activity not related to the surface area, O<sub>2</sub> evolution of CNR was increased to a rate of 7 µmol/h, keeping all other parameters unaltered.<sup>122</sup> The photocatalytic H<sub>2</sub> evolution activity of CNRs is also improved by a factor of ~3 over bulk g-C<sub>3</sub>N<sub>4</sub>. The photocurrent output and H<sub>2</sub>-revolution rate of CNR were also enhanced, which we attribute to the improvement of condensation and orientation within the high-aspect-ratio nanowire structures.

As mentioned in Section 4, the electronic structure of the g-C<sub>3</sub>N<sub>4</sub> can be additionally adjusted through doping of heteroatoms. For example, already, the UV–vis spectrum indicates that fluorine doping gives rise to a decrease in the band gap from 2.69 eV for g-C<sub>3</sub>N<sub>4</sub> to 2.63 eV for CNF-2.0. Indeed, the H<sub>2</sub> evolution of CNF-0.5 was ~2.7 times higher than that of unmodified g-C<sub>3</sub>N<sub>4</sub>.<sup>38</sup> Another typical example is the modification of the polymeric subunits by copolymerization with barbituric acid.<sup>99</sup> These copolymerization products show a remarkable red shift of optical absorption compared with g-C<sub>3</sub>N<sub>4</sub> from 470 to 750 nm with increasing barbituric acid content and an improvement in H<sub>2</sub> evolution activity both under UV

irradiation and, especially, with visible light. The maximal H<sub>2</sub> evolution activity comes from the most weakly doped sample, which shows a 4.5 times higher activity than that of unmodified g-C<sub>3</sub>N<sub>4</sub>.

Cheng and co-workers have found that the sulfur-doped carbon nitride displays an electronic structure with an increased valence bandwidth in combination with an elevated conduction band minimum and a slightly reduced absorbance.<sup>44</sup> These features result collectively in a unique electronic structure that is highly efficient in promoting visible light photoreduction. This sulfur-doped carbon nitride shows improved photocatalytic activity evolution from an aqueous triethanolamine solution; the photoactivity of H<sub>2</sub> evolution is 7.2 and 8.0 times higher than that of bare g-C<sub>3</sub>N<sub>4</sub> under >300 and 420 nm, respectively.

Following a related strategy, our group found that a sulfur-mediated synthesis offers an effective approach to modify the texture and the optical and electronic properties as well as the photoreduction and photo-oxidation.<sup>45</sup> Contrary to other modifications, sulfur-mediated synthesis even lowers the HOMO of the organic semiconductor structure; that is, it makes it more stable and, therefore, the hole in the band structure more oxidative. In perfect agreement with these general quantum chemical considerations, the water oxidation reaction has been achieved at a moderate rate, even with only sulfur-mediated carbon nitride without the aid of cofactors (Figure 10). This material is therefore a stronger and more efficient oxidation catalyst.

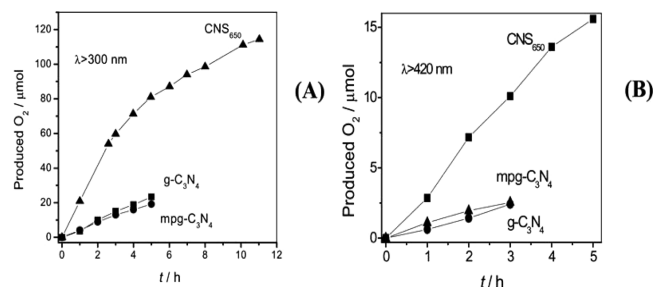


**Figure 10.** Oxygen evolution by g-C<sub>3</sub>N<sub>4</sub>, mpg-C<sub>3</sub>N<sub>4</sub>, and CNS<sub>650</sub> as a function of time under (A) UV and (B) visible light illumination.

Another strategy to extend the photoresponse of carbon nitride to the visible region is to harvest visible light by adsorbed dyes. In this strategy, the dyes act as antennas to absorb and transfer the light energy into the reaction system. In the case of appropriately chosen band positions, the photochemical reactions could be initiated through electron transfer from the excited states of the dye into the conduction band of carbon nitride, leaving the hole well separated at the dye structure. For example, Domen and co-workers deposited magnesium phthalocyanine (MgPc) onto the mpg-C<sub>3</sub>N<sub>4</sub> which expands the absorption to the Q-band (Figure 11).<sup>123</sup> The as-obtained MgPc/Pt/mpg-C<sub>3</sub>N<sub>4</sub> showed stable photocatalytic evolution of hydrogen from an aqueous solution containing TEOA as a sacrificial reagent, resulting in a quantum efficiency of ~5.6% at 420 nm. It is worth noting that the photocatalytic test gave hydrogen evolution even when irradiated at a wavelength longer than 600 nm.

**5.2. Carbon Nitride As a Catalyst for Organic Oxidation/Dehydrogenation Reactions.** Catalytic oxidation is an important method for bringing functionality into both petroleum- and biomass-based feedstocks because it is often the

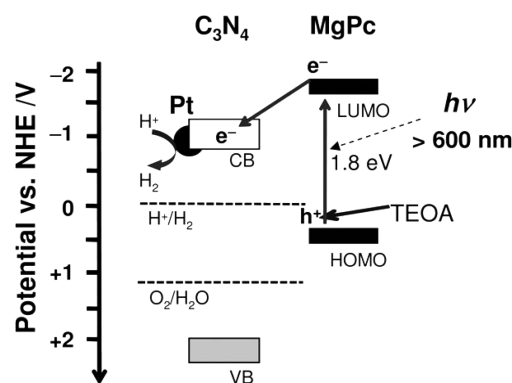


**Figure 11.** Scheme of electron–hole separation in MgPc/Pt/mpg-C<sub>3</sub>N<sub>4</sub> photocatalysts. Band positions of mpg-C<sub>3</sub>N<sub>4</sub> were determined by photoelectron emission spectroscopy in air and UV–vis DRS.

first step to high-value fine chemicals, agrochemicals, and pharmaceuticals.<sup>124</sup> The oxidation of primary alcohols to aldehydes is one of those elementary reactions that are of fundamental importance in both the laboratory and commercial procedures. Many oxidations of this type are carried out using corrosive and stoichiometric oxygen donors such as chromate or permanganate and generally transition-metal catalysts.<sup>125,126</sup> In recent years, heterogeneous photocatalysis developed to a promising method for numbers of chemical reactions at the expense of solar energy.<sup>127,128</sup> As mentioned above, g-C<sub>3</sub>N<sub>4</sub> has an appropriate band gap and also band positions. This feature allows its direct use in photochemical activation of O<sub>2</sub> and the organic compounds in which g-C<sub>3</sub>N<sub>4</sub> was used as a photocatalyst to absorb light, with the generated charge couple to activate oxygen.

This photocatalysis system can be easily applied to the oxidation of alcohols. Recent work shows that light-excited mesoporous g-C<sub>3</sub>N<sub>4</sub> can activate molecular oxygen for the oxidation of alcohols to aldehydes/ketones with high selectivity.<sup>132</sup> Mesoporous mpg-C<sub>3</sub>N<sub>4</sub> catalyzes the oxidation of benzyl alcohol to benzaldehyde with >99% selectivity and 57% conversion under visible light irradiation for 3 h at 100 °C (Table 1). A study on the effect of substitution on the aromatic ring shows both the electron-withdrawing and electron-donating substituent enhanced the rate of the reaction, as listed in Table 1.

**Table 1. Selective Oxidation of Alcohols**

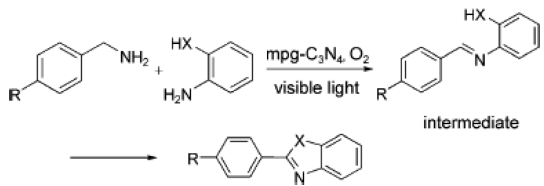
$\text{R}_1-\text{CH}_2-\text{CH}(\text{OH})-\text{R}_2 \xrightarrow[\text{light, trifluorotoluene}]{\text{mpg-C}_3\text{N}_4, \text{O}_2 (8 \text{ bar}), 100 \text{ }^\circ\text{C}}$		$\text{R}_1-\text{CH}_2-\text{C}(=\text{O})-\text{R}_2$			
R <sup>1</sup>	R	time, h	concn, %	selectivity, %	
1	phenyl	CH <sub>3</sub>	3	57	>99
2	phenyl	H	3	77	>99
3	4-methylphenyl	H	3	86	90 <sup>a</sup>
4	4-chlorophenyl	H	3	79	>99
5 <sup>b</sup>	4-methoxyphenyl	H	1.8	100	95 <sup>c</sup>
6	4-methylbenzoate	H	3	80	>99
7	PhCH=CH <sub>2</sub>	H	3	92	64 <sup>d</sup>
8	pentyl	CH <sub>3</sub>	5	35	>99
9	phenyl	cyclopropyl	5	32	90 <sup>d</sup>

<sup>a</sup>Acid (10%) was formed. <sup>b</sup>4-Methoxybenzyl alcohol 0.65 mmol. <sup>c</sup>Acid (5%) was formed. <sup>d</sup>Benzaldehyde (36%) was detected. <sup>e</sup>1-(1,2-Dicyclopropyl-2-phenylethyl)benzene (10%) was formed.

Complementary electron spin resonance (ESR) experiments suggested the formation of the  $\cdot\text{O}_2^-$  radical by electron transfer from the photoactivated  $\text{mpg-C}_3\text{N}_4$  under visible light irradiation, whereas the cationic hole directly dehydrogenates the alcohol (oxidative dehydrogenation). The whole reaction is clearly surface-mediated; that is, the  $\cdot\text{O}_2^-$  stays excitonically coupled to its counterion radical.

Apart from C–H and O–H oxidation, N–H oxidation is of considerable interest because it allows generation of a number of active nitrogen-containing compounds as intermediates of various chemically and biologically significant molecules.  $\text{mpg-C}_3\text{N}_4$  can also promote the oxidative dehydrogenation of amines into imines under the illumination of visible light, which then immediately undergo consecutive reactions. Under optimized conditions, complete conversion of benzylamine into *N*-benzylidene benzylamine was obtained in 3.5 h. Note this strategy was successfully extended to other substrates, such as heterocyclic amines containing nitrogen and sulfur atoms. This is a rare catalytic reaction, as these heteroatoms usually poison most metal catalysts. Specifically, a simple and efficient synthesis of benzoxazoles, benzimidazoles, and benzothiazoles could be realized through a one-pot synthesis by this photocatalytic cascade reaction with notably high yields (Table 2).<sup>129</sup>

**Table 2. One-Pot Aerobic Coupling Synthesis of Benzoxaoles, Benzimidazoles, And Benzothiazoles**



entry	R	X	<i>t</i> , h	conversion, % <sup>b</sup>	selectivity, % <sup>b</sup>
1	CH <sub>3</sub>	O	5	99	69
2	H	O	5	99	75
3 <sup>d</sup>	H	O	5	99	24
4	Cl	O	5	70	74
5	CH <sub>3</sub>	NCH <sub>3</sub>	4	97	92
6	H	NCH <sub>3</sub>	5	99	98
7	Cl	NCH <sub>3</sub>	5.5	98	91
8	OCH <sub>3</sub>	S	4	96	97
9	H	S	5	91	92
10	Cl	S	5.5	97	93

<sup>a</sup>Reaction conditions: substituted benzylamine (1 mmol),  $\text{mpg-C}_3\text{N}_4$  catalyst (50 mg), 2-aminophenol (2-aminothiophenol or *o*-phenylenediamine) (3 mmol), CH<sub>3</sub>CN (10 mL), 100 °C, O<sub>2</sub> (0.5 MPa).  
<sup>b</sup>Conversion and selectivity were based on benzylamines <sup>a</sup>80 °C; using the main product of 2-hydroxybenzoinmine.

After successful implication of  $\text{mpg-C}_3\text{N}_4$  in photoredox conversion of a broad scope of primary and secondary amine substrates, the photocatalytic scheme was extended to the oxidation of tertiary amines. On the basis of the reaction mechanism of primary and secondary amine substrates, it is assumed that iminium ions could also be generated in a similar way in the reaction of tertiary amines. The generated iminium ions as highly reactive intermediates can undergo further catalytic tandem transformations under photoredox conditions (Figure 12).

Indeed, the oxidative coupling of *N*-phenyl-1,2,3,4-tetrahydroisoquinoline with nitromethane in the presence of  $\text{mpg-C}_3\text{N}_4$ , visible light, and oxygen can achieve 100% conversion to the

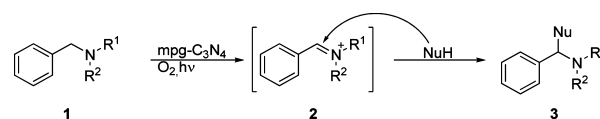
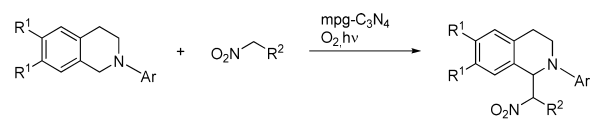


**Figure 12.** Photocatalytic oxidative Mannich reaction.

desired product at a high isolated yield of 92%. Oxidative coupling reactions of various tetrahydroisoquinolines with nitroalkanes have also been demonstrated (Table 3).

**Table 3. Oxidative Coupling Reactions of Various Tetrahydroisoquinolines with Nitroalkanes<sup>a</sup>**



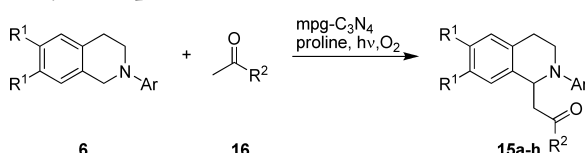
Entry	R <sup>1</sup>	Ar	R <sup>2</sup>	product	yield [%] <sup>c</sup>
1	H	Ph	H	8a	92
2	H	Ph	Me	8b	81
3	H	Ph	Et	8c	91
4	H	<i>p</i> Tol	H	8d	85
5	H	<i>p</i> Tol	Me	8e	86
6	H	<i>p</i> MeO-Ph	H	8f	89
7	H	<i>p</i> MeO-Ph	Me	8g	91
8	OMe	Ph	H	8h	91
9	OMe	Ph	Me	8i	83
10 <sup>a</sup>	H	<i>p</i> Cl-Ph	H	8j	88
11 <sup>a</sup>	H	<i>p</i> Br-Ph	H	8k	92
12	H	<i>p</i> <sup>t</sup> Bu-Ph	H	8l	92
13 <sup>b</sup>			H		36

<sup>a</sup>Reaction conditions: rt, 0.25 mmol substrate, 1 mL MeCN, 5 equiv nucleophile, 15 mg  $\text{mpg-C}_3\text{N}_4$ , 22–34 h, 60 W energy-saving bulb, 1 bar O<sub>2</sub>; (a) MeNO<sub>2</sub> was used as solvent instead of MeCN; (b) reaction time: 92 h; (c) isolated yield after chromatography on SiO<sub>2</sub>.

It is of particular interest that this visible light photoredox catalysis scheme can be further integrated with proline organocatalysis to achieve catalytic oxidative cascade reactions, opening a new avenue in Mannich chemistry.<sup>135</sup> That way, a series of highly relevant synthetic intermediates could be realized (Table 4).

**5.3. Photodegradation of Pollutants.** The oxidation of the organic pollutants into CO<sub>2</sub>, water, and other nonhazardous compounds using O<sub>2</sub> as a clean oxidant is one of the few effective approaches to remove the organic pollutants rapidly and in an environmentally friendly manner.<sup>130</sup> Recently, Zou and co-workers were able to degrade methyl orange (MO) and



**Table 4. Dual Catalytic Mannich Reaction of Various Tetrahydroisoquinolines<sup>a</sup>**


entry	R <sup>1</sup>	Ar	R <sup>2</sup>	product	yield, % <sup>b</sup>
1	H	Ph	Me	15a	94
2	H	Ph	Et	15b	44
3	H	<i>p</i> Tol	Me	15c	80
4	H	<i>p</i> MeO-Ph	Me	15d	78
5	H	<i>p</i> <sup>t</sup> Bu-Ph	Me	15e	71
6	H	<i>p</i> Br-Ph	Me	15f	88
7	OMe	Ph	Me	15g	73
8	H	<i>m</i> CF <sub>3</sub> -Ph	Me	15h	61

<sup>a</sup>Reaction conditions: rt, 0.25 mmol substrate, 1 mL proline, 20 mol % proline, 15 mg mpg-C<sub>3</sub>N<sub>4</sub>, 22–34 h, 60 W energy-saving bulb, 1 bar O<sub>2</sub>. <sup>b</sup>Isolated yield after chromatography on SiO<sub>2</sub>.

rhodamine B (RhB) using g-C<sub>3</sub>N<sub>4</sub> as a metal-free photocatalyst.<sup>94</sup> Their comparison studies showed that the photodegradation activity of MO over g-C<sub>3</sub>N<sub>4</sub> is attributed mainly to the reduction process initiated by photogenerated electrons, whereas the degradation of RhB over g-C<sub>3</sub>N<sub>4</sub> originated mainly from the oxidation by the photogenerated hole. Boron doping for g-C<sub>3</sub>N<sub>4</sub> can improve the dye adsorption and light absorption and therefore promote the photodegradation of RhB.<sup>30</sup> The same group also fabricated a C<sub>3</sub>N<sub>4</sub>–TaON composite photocatalyst by the milling-heat treatment method. This organic–inorganic heterojunction has a good performance in the photooxidation of RhB which resulted from the suitably matching conduction and valence band levels that improved the separation efficiency of photogenerated electron–hole pairs (Figure 13).<sup>131</sup>

The carbon nitride polymer has also been applied as a metal-free photocatalyst to activate H<sub>2</sub>O<sub>2</sub> under visible light irradiation to produce ·OH for the degradation of organic pollutants in water. The conversion of RhB into CO<sub>2</sub> was taken as a model system.<sup>133</sup> The system was stable against photocorrosion, even in

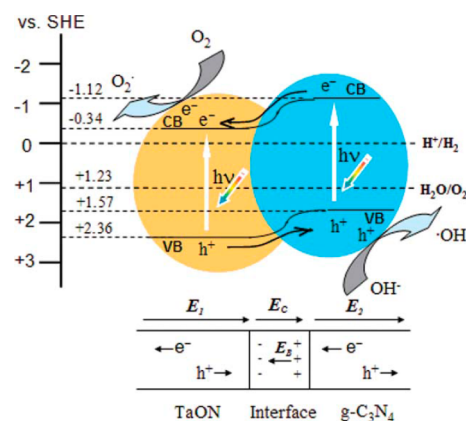


**Figure 13.** Scheme for electron–hole separation and transport at the visible-light-driven organic–inorganic composite photocatalyst interface and in both semiconductors:  $E_C$  is the contact electric field for the two materials;  $E_B$  is the potential barrier in the interfacial depletion layer ( $E_B < E_C$  during a photocatalytic reaction);  $E_1$  and  $E_2$  are the internal electric fields induced by the redistribution of the spatial charges in TaON and C<sub>3</sub>N<sub>4</sub> particles, respectively.

the presence of H<sub>2</sub>O<sub>2</sub>, and after five repeated operations, there was no noticeable deactivation of carbon nitride photocatalysts. This photocatalytic process for the activation of H<sub>2</sub>O<sub>2</sub> avoids the employment of any metal derivatives, and the catalyst was found to be stable and reusable (see Figure 14), creating promise for environmental cleanup of organic pollutants in water.

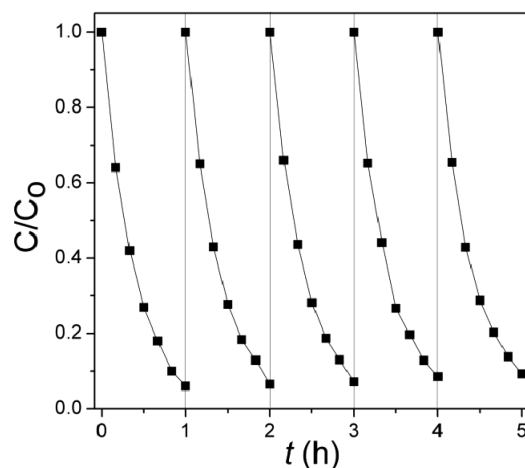


**Figure 14.** The cycling runs of the degradation of RhB (10<sup>-5</sup> M) in the g-C<sub>3</sub>N<sub>4</sub>/H<sub>2</sub>O<sub>2</sub> (0.08 M) system under visible light irradiation. Reprint from ref 133, copyright 2012, Royal Society of Chemistry.

## 6. CONCLUSIONS AND OUTLOOK

Since the first use of g-C<sub>3</sub>N<sub>4</sub> as a metal-free heterogeneous catalyst in 2006,<sup>93,94</sup> studies on the catalytical, electrocatalytical, and photocatalytical performance of carbon nitride have been steadily increasing. In this Perspective, we have presented some approaches to make and structure such catalysts and have introduced the special role of g-C<sub>3</sub>N<sub>4</sub> in photocatalysis. It is the peculiarity of modified carbon nitrides that they are heterogeneous organocatalysts; that is, they catalyze reactions by organic interactions and activation schemes. In addition, carbon nitride is a medium band gap semiconductor, with both the HOMO and LUMO positions in a range that makes it a mild electron transfer agent with powerful chemical potential.

As mentioned above, in many examples, carbon nitride or its modifications have already provided new opportunities in practical applications, including artificial photosynthesis, oxygenation, and hydrogen transfer reactions. Compared with traditional heterogeneous catalysts or catalyst supports, carbon nitride has many advantages, such as being metal-free, showing good thermal and chemical stability, tunable electronic structure, and being abundant and inexpensive. Therefore, one can foresee intensified interest in carbon nitride for green chemistry, but further systematic work is needed. The catalytic rates of carbon nitride were still rather low when metal-free carbon nitride was used, and this was attributed to the role of covalence in the reversible bonds to be formed and split with the catalyst.

Going forward, we believe that “enzyme-like” multifunctional modifications of carbon nitrides, best in the form of functional pores, are a way to improve the performance of metal-free carbon nitride. Another target should be to establish the correlations between the carbon nitride structures and the catalytically active structure in the relevant reactions. It is still not very clear how the carbon nitride interacts with the reactants and the products and how the carbon nitride really influences the relevant reactions.

To reach a more fundamental level, a basic understanding of physicochemical properties of carbon nitride is needed.

Because the organic chemistry of C–N bond formation is very rich, we also expect the advent of better, milder, and more reversible synthesis protocols of diverse C/N-scaffolded structures that also enable self-organization toward improved structure motifs.

From the perspective of practical applications in sustainable chemistry, only a few reactions have been addressed until now, which, however, underline the requested tolerance against multifunctionality and water. Applying this catalyst to specific key reactions and specific substrates will certainly create more exciting results in the near future.

## AUTHOR INFORMATION

### Corresponding Author

\*E-mail: office.cc@mpikg.mpg.de.

### Present Address

†Institute of Chemistry, Technical University Berlin, Strasse des 17, Juni 135, 10623 Berlin, Germany

### Notes

The authors declare no competing financial interest.

## ACKNOWLEDGMENTS

The authors are grateful to the EnerChem project of the Max Planck Society, the National Natural Science Foundation of China (Nos. 21033003 and 21173043), and all the research partners involved in the previous projects. Special thanks also goes to UNICAT, the German excellence initiative on catalysis at TU Berlin, which enabled an effective interdisciplinary approach.

## REFERENCES

- (1) Liebig, J. V. *Ann. Pharm.* **1834**, *10*, 10.
- (2) Benard, D. J.; Linnen, C.; Harker, A.; Michels, H. H.; Addison, J. B.; Ondercin, R. *J. Phys. Chem. B* **1998**, *102*, 6010.
- (3) Bai, X. J.; Cao, C. B.; Xu, X. Y.; Yu, Q. A. *Solid State Commun.* **2010**, *150*, 2148.
- (4) Bai, X. J.; Cao, C. B.; Xu, X. Y. *Mater. Sci. Eng., B* **2010**, *175*, 95.
- (5) Wasche, R.; Hartelt, M.; Springborn, U.; Bewilogua, K.; Keunecke, M. *Wear* **2010**, *269*, 816.
- (6) Naffakh, M.; Lopez, V.; Zamora, F.; Gomez, M. A. *Soft Mater.* **2010**, *8*, 407.
- (7) Xia, X.; Zhou, C. H.; Tong, D. S.; Liu, M.; Zhang, D.; Fang, M.; Yu, W. H. *Mater. Lett.* **2010**, *64*, 2620.
- (8) Tokoroyama, T.; Umehara, N.; Kamiya, M.; Fuwa, Y. *Jpn. Soc. Tribol.* **2010**, *55*, 659.
- (9) Shalaev, R. V.; Ulyanov, A. N.; Prudnikov, A. M.; Shin, G. M.; Yoo, S. I.; Varyukhin, V. N. *Phys. Status Solidi A* **2010**, *207*, 2300.
- (10) Jiang, G. F.; Zhou, C. H.; Xia, X.; Yang, F. Q.; Tong, D. S.; Yu, W. H.; Liu, S. M. *Mater. Lett.* **2010**, *64*, 2718.
- (11) Byers, J. C.; Tamiasso-Martinhon, P.; Deslouis, C.; Pailleret, A.; Semenikhin, O. A. *J. Phys. Chem. C* **2010**, *114*, 18474.
- (12) Banerjee, I.; Kumari, N.; Singh, A. K.; Kumar, M.; Laha, P.; Panda, A. B.; Pabi, S. K.; Barhai, P. K.; Mahapatra, S. K. *Thin Solid Films* **2010**, *518*, 7240.
- (13) Liu, D. G.; Tu, J. P.; Hong, C. F.; Gu, C. D.; Mao, S. X. *Surf. Coat. Technol.* **2010**, *205*, 152.
- (14) Ben Karoui, M.; Gharbi, R.; Elzayed, N.; Fathallah, M.; Tresso, E. In *Proceedings of the JMSM 2008 Conference*; Cheikhrouhou, A., Ed.; 2009; Vol. 2, p 873.
- (15) Bian, S. W.; Ma, Z.; Song, W. G. *J. Phys. Chem. C* **2009**, *113*, 8668.
- (16) Kroke, E.; Schwarz, M. *Coord. Chem. Rev.* **2004**, *248*, 493.
- (17) Vinu, A. *Adv. Funct. Mater.* **2008**, *18*, 816.
- (18) Ito, H.; Nozaki, T.; Saikubo, A.; Yamada, N.; Kanda, K.; Niibe, M.; Saitoh, H. *Thin Solid Films* **2008**, *516*, 6575.

- (19) Yang, S. J.; Cho, J. H.; Oh, G. H.; Nahm, K. S.; Park, C. R. *Carbon* **2009**, *47*, 1585.
- (20) Bai, X. D.; Zhong, D. Y.; Zhang, G. Y.; Ma, X. C.; Liu, S.; Wang, E. G.; Chen, Y.; Shaw, D. T. *Appl. Phys. Lett.* **2001**, *79*, 1552.
- (21) Li, Q. A.; Yang, J. P.; Feng, D.; Wu, Z. X.; Wu, Q. L.; Park, S. S.; Ha, C. S.; Zhao, D. Y. *Nano Res.* **2010**, *3*, 632.
- (22) Haque, E.; Jun, J. W.; Talapaneni, S. N.; Vinu, A.; Jung, S. H. *J. Mater. Chem.* **2010**, *20*, 10801.
- (23) Zhou, Z. B.; Cui, R. Q.; Pang, Q. J.; Hadi, G. M.; Ding, Z. M.; Li, W. Y. *Solar Energy Mater. Solar Cells* **2002**, *70*, 487.
- (24) Zhang, Y. J.; Antonietti, M. *Chem.—Asian J.* **2010**, *5*, 1307.
- (25) Di Noto, V.; Negro, E. *Electrochim. Acta* **2010**, *55*, 7564.
- (26) Lee, S. P.; Lee, J. G.; Chowdhury, S. *Sensors* **2008**, *8*, 2662.
- (27) Lee, S. P. *Sensors* **2008**, *8*, 1508.
- (28) Thomas, A.; Fischer, A.; Goettmann, F.; Antonietti, M.; Muller, J. O.; Schlogl, R.; Carlsson, J. M. *J. Mater. Chem.* **2008**, *18*, 4893.
- (29) Wang, Y.; Zhang, J. S.; Wang, X. C.; Antonietti, M.; Li, H. R. *Angew. Chem., Int. Ed.* **2010**, *49*, 3356.
- (30) Yan, S. C.; Li, Z. S.; Zou, Z. G. *Langmuir* **2010**, *26*, 3894.
- (31) Miyamoto, Y.; Cohen, M. L.; Louie, S. G. *Solid State Commun.* **1997**, *102*, 605.
- (32) Horvath-Bordon, E.; Kroke, E.; Svoboda, I.; Fuess, H.; Riedel, R. *New J. Chem.* **2005**, *29*, 693.
- (33) Bai, Y. J.; Lu, B.; Liu, Z. G.; Li, L.; Cui, D. L.; Xu, X. G.; Wang, Q. L. *J. Cryst. Growth* **2003**, *247*, 505.
- (34) Zhao, Y. C.; Liu, Z.; Chu, W. G.; Song, L.; Zhang, Z. X.; Yu, D. L.; Tian, Y. J.; Xie, S. S.; Sun, L. F. *Adv. Mater.* **2008**, *20*, 1777.
- (35) Groenewolt, M.; Antonietti, M. *Adv. Mater.* **2005**, *17*, 1789.
- (36) Komatsu, T.; Nakamura, T. *J. Mater. Chem.* **2001**, *11*, 474.
- (37) Li, X. F.; Zhang, J.; Shen, L. H.; Ma, Y. M.; Lei, W. W.; Cui, Q. L.; Zou, G. T. *Appl. Phys. A: Mater. Sci. Process.* **2009**, *94*, 387.
- (38) Wang, Y.; Di, Y.; Antonietti, M.; Li, H. R.; Chen, X. F.; Wang, X. C. *Chem. Mater.* **2010**, *22*, 5119.
- (39) Antonietti, M.; Fratzl, P. *Macromol. Chem. Phys.* **2010**, *211*, 166.
- (40) Wang, X. C.; Maeda, K.; Thomas, A.; Takanabe, K.; Xin, G.; Carlsson, J. M.; Domen, K.; Antonietti, M. *Nat. Mater.* **2009**, *8*, 76.
- (41) Wang, Y.; Li, H. R.; Yao, J.; Wang, X. C.; Antonietti, M. *Chem. Sci.* **2011**, DOI: 10.1039/C0SC00475H.
- (42) Yan, S. C.; Li, Z. S.; Zou, Z. G. *Langmuir* **2009**, *25*, 10397–10401.
- (43) Zhang, Y. J.; Thomas, A.; Antonietti, M.; Wang, X. C. *J. Am. Chem. Soc.* **2009**, *131*, 50.
- (44) Liu, G.; Niu, P.; Sun, C. H.; Smith, S. C.; Chen, Z. G.; Lu, G. Q.; Cheng, H. M. *J. Am. Chem. Soc.* **2010**, *132*, 11642.
- (45) Zhang, J. H.; Sun, J. H.; Maeda, K.; Domen, K.; Liu, P.; Antonietti, M.; Fu, X. Z.; Wang, X. C. *Energy Environ. Sci.* **2011**, DOI: 10.1039/c0ee00418.
- (46) Semench, A. V.; Blinov, L. N. *Glass Phys. Chem.* **2010**, *36*, 199–208.
- (47) Franklin, E. C. *J. Am. Chem. Soc.* **1922**, *44*, 486.
- (48) Pauling, L.; Sturdivant, J. H. *Proc. Natl. Acad. Sci. U. S. A.* **1937**, *23*, 615.
- (49) Redemann, C. E.; Lucas, H. J. *J. Am. Chem. Soc.* **1940**, *62*, 842.
- (50) Cohen, M. L. *Phys. Rev. B* **1985**, *32*, 7988.
- (51) Liu, A. Y.; Cohen, M. L. *Science* **1989**, *245*, 841.
- (52) Cohen, M. L. *Science* **1993**, *261*, 307.
- (53) Teter, D. M.; Hemley, R. J. *Science* **1996**, *271*, 53.
- (54) Corkill, J. L.; Cohen, M. L. *Phys. Rev. B* **1993**, *48*, 17622.
- (55) Maya, L.; Cole, D. R.; Hagan, E. W. *J. Am. Ceram. Soc.* **1991**, *74*, 1686–1688.
- (56) Nesting, D. C.; Badding, J. V. *Chem. Mater.* **1996**, *8*, 1535.
- (57) Liu, A. Y.; Wentzcovitch, R. M. *Phys. Rev. B* **1994**, *50*, 10362.
- (58) Lowther, J. E. *Phys. Rev. B* **1999**, *59*, 11683.
- (59) Ortega, J.; Sankey, O. F. *Phys. Rev. B* **1995**, *51*, 2624.
- (60) Bojdys, M. J.; Muller, J. O.; Antonietti, M.; Thomas, A. *Chem.—Eur. J.* **2008**, *14*, 8177–8182.
- (61) Jurgens, B.; Irran, E.; Senker, J.; Kroll, P.; Muller, H.; Schnick, W. *J. Am. Chem. Soc.* **2003**, *125*, 10208.
- (62) Seyfarth, L.; Seyfarth, J.; Lotsch, B. V.; Schnick, W.; Senker, J. *Phys. Chem. Chem. Phys.* **2010**, *12*, 2227.

- (63) Sattler, A.; Pagano, S.; Zeuner, M.; Zurawski, A.; Gunzelmann, D.; Senker, J.; Müller-Buschbaum, K.; Schnick, W. *Chem.—Eur. J.* **2009**, *15*, 13161.
- (64) Doeblinger, M.; Lotsch, B. V.; Wack, J.; Thun, J.; Senker, J.; Schnick, W. *Chem. Commun.* **2009**, 1541.
- (65) Sattler, A.; Schnick, W. *Z. Anorg. Allg. Chem.* **2008**, *634*, 457.
- (66) Miller, D. R.; Wang, J. J.; Gillan, E. G. *J. Mater. Chem.* **2002**, *12*, 2463.
- (67) Zou, X.-X.; Li, G.-D.; Wang, Y.-N.; Zhao, J.; Yan, C.; Guo, M.-Y.; Li, L.; Chen, J.-S. *Chem. Commun.* **2011**, *47*, 1066.
- (68) Matsumoto, S.; Xie, E. Q.; Izumi, F. *Diamond Relat. Mater.* **1999**, *8*, 1175.
- (69) Kouvetakis, J.; Bandari, A.; Todd, M.; Wilkens, B.; Cave, N. *Chem. Mater.* **1994**, *6*, 811.
- (70) Li, C.; Cao, C. B.; Zhu, H. S. *Mater. Lett.* **2004**, *58*, 1903.
- (71) Lotsch, B. V.; Schnick, W. *Chem. Mater.* **2006**, *18*, 1891.
- (72) Young-Gui, Y.; Pfrommer, B. G.; Mauri, F.; Louie, S. G. *Phys. Rev. Lett.* **1998**, *80*, 3388.
- (73) Molina, B.; Sansores, L. E. *Mod. Phys. Lett. B* **1999**, *13*, 193.
- (74) Alves, I.; Demazeau, G.; Tanguy, B.; Weill, F. *Solid State Commun.* **1999**, *109*, 697.
- (75) Zhang, Z. H.; Leinenweber, K.; Bauer, M.; Garvie, L. A. J.; McMillan, P. F.; Wolf, G. H. *J. Am. Chem. Soc.* **2001**, *123*, 7788.
- (76) Mattesini, M.; Matar, S. F.; Snis, A.; Etourneau, J.; Mavromaras, A. *J. Mater. Chem.* **1999**, *9*, 3151.
- (77) Snis, A.; Matar, S. F. *Phys. Rev. B* **1999**, *60*, 10855.
- (78) Courjault, S.; Tanguy, B.; Demazeau, G. *C. R. Acad. Sci. Series II Fascicule C, Chim.* **1999**, *2*, 487.
- (79) Montigaud, H.; Tanguy, B.; Demazeau, G.; Alves, I.; Birot, M.; Dunogues, J. *Diamond Relat. Mater.* **1999**, *8*, 1707.
- (80) Khabashesku, V. N.; Zimmerman, J. L.; Margrave, J. L. *Chem. Mater.* **2000**, *12*, 3264.
- (81) Zimmerman, J. L.; Williams, R.; Khabashesku, V. N.; Margrave, J. L. *Nano Lett.* **2001**, *1*, 731.
- (82) Kroke, E.; Schwarz, M.; Horath-Bordon, E.; Kroll, P.; Noll, B.; Norman, A. D. *New J. Chem.* **2002**, *26*, 508.
- (83) Rignanese, G. M.; Charlier, J. C.; Gonze, X. *Phys. Rev. B* **2002**, *66*, 205416.
- (84) Zhang, Y.; Sun, H.; Chen, C. F. *Phys. Rev. B* **2006**, *73*.
- (85) Gmelin, L. *Ann. Pharm.* **1835**, *15*, 252.
- (86) Liebig, J. V. *Ann. Chem. Pharm.* **1850**, *50*, 337.
- (87) Liebig, J. V. *Ann. Chem. Pharm.* **1850**, *73*, 257.
- (88) May, H. J. *Appl. Chem.* **1959**, 340.
- (89) Sehnert, J.; Baerwinkel, K.; Senker, J. *J. Phys. Chem. B* **2007**, *111*, 10671.
- (90) Lotsch, B. V.; Schnick, W. *Chem.—Eur. J.* **2007**, *13*, 4956.
- (91) Komatsu, T. *J. Mater. Chem.* **2001**, *11*, 799.
- (92) Komatsu, T. *J. Mater. Chem.* **2001**, *11*, 802.
- (93) Goettmann, F.; Fischer, A.; Antonietti, M.; Thomas, A. *Angew. Chem., Int. Ed.* **2006**, *45*, 4467.
- (94) Goettmann, F.; Fischer, A.; Antonietti, M.; Thomas, A. *Chem. Commun.* **2006**, 4530.
- (95) Gillan, E. G. *Chem. Mater.* **2000**, *12*, 3906.
- (96) Kawaguchi, M.; Nozaki, K. *Chem. Mater.* **1995**, *7*, 257.
- (97) Deifallah, M.; McMillan, P. F.; Cora, F. J. *Phys. Chem. C* **2008**, *112*, 5447.
- (98) Wang, J. J.; Miller, D. R.; Gillan, E. G. *Chem. Commun.* **2002**, 2258.
- (99) Zhang, J. S.; Chen, X. F.; Takanabe, K.; Maeda, K.; Domen, K.; Epping, J. D.; Fu, X. Z.; Antonietti, M.; Wang, X. C. *Angew. Chem., Int. Ed.* **2010**, *49*, 441.
- (100) Zhang, M.; Nakayama, Y.; Harada, S. *J. Appl. Phys.* **1999**, *86*, 4971.
- (101) Wang, X. C.; Maeda, K.; Chen, X. F.; Takanabe, K.; Domen, K.; Hou, Y. D.; Fu, X. Z.; Antonietti, M. *J. Am. Chem. Soc.* **2009**, *131*, 1680.
- (102) Polarz, S.; Antonietti, M. *Chem. Commun.* **2002**, 2593.
- (103) Liang, C. D.; Hong, K. L.; Guiochon, G. A.; Mays, J. W.; Dai, S. *Angew. Chem., Int. Ed.* **2004**, *43*, 5785.
- (104) Thomas, A.; Goettmann, F.; Antonietti, M. *Chem. Mater.* **2008**, *20*, 738.
- (105) Jun, Y. S.; Hong, W. H.; Antonietti, M.; Thomas, A. *Adv. Mater.* **2009**, *21*, 4270.
- (106) Chen, X. F.; Jun, Y. S.; Takanabe, K.; Maeda, K.; Domen, K.; Fu, X. Z.; Antonietti, M.; Wang, X. C. *Chem. Mater.* **2009**, *21*, 4093.
- (107) Antonietti, M. *Curr. Opin. Colloid Interface Sci.* **2001**, *6*, 244.
- (108) Chen, D. H.; Li, Z.; Wan, Y.; Tu, X. J.; Shi, Y. F.; Chen, Z. X.; Shen, W.; Yu, C. Z.; Tu, B.; Zhao, D. Y. *J. Mater. Chem.* **2006**, *16*, 1511.
- (109) Liang, C. D.; Li, Z. J.; Dai, S. *Angew. Chem., Int. Ed.* **2008**, *47*, 3696.
- (110) Meng, Y.; Gu, D.; Zhang, F. Q.; Shi, Y. F.; Cheng, L.; Feng, D.; Wu, Z. X.; Chen, Z. X.; Wan, Y.; Stein, A.; Zhao, D. Y. *Chem. Mater.* **2006**, *18*, 4447.
- (111) Kosonen, H.; Valkama, S.; Nykanen, A.; Toivanen, M.; ten Brinke, G.; Ruokolainen, J.; Ikkala, O. *Adv. Mater.* **2006**, *18*, 201.
- (112) Wang, Y.; Wang, X. C.; Antonietti, M.; Zhang, Y. J. *ChemSusChem* **2010**, *3*, 435–439.
- (113) Zhang, Y. J.; Mori, T.; Ye, J. H.; Antonietti, M. *J. Am. Chem. Soc.* **2010**, *132*, 6294.
- (114) Wang, Y.; Li, H. R.; Yao, J.; Wang, X. C.; Antonietti, M. *Chem. Sci.* **2011**, *2*, 446–450.
- (115) Ritterskamp, P.; Kuklya, A.; Wustkamp, M. A.; Kerpen, K.; Weidenthaler, C.; Demuth, M. *Angew. Chem., Int. Ed.* **2007**, *46*, 7770.
- (116) Kohl, S. W.; Weiner, L.; Schwartsburd, L.; Konstantinovski, L.; Shimon, L. J. W.; Ben-David, Y.; Iron, M. A.; Milstein, D. *Science* **2009**, *324*, 74.
- (117) Kudo, A.; Miseki, Y. *Chem. Soc. Rev.* **2009**, *38*, 253.
- (118) Osterloh, F. E. *Chem. Mater.* **2008**, *20*, 35.
- (119) Maeda, K.; Wang, X. C.; Nishihara, Y.; Lu, D. L.; Antonietti, M.; Domen, K. *J. Phys. Chem. C* **2009**, *113*, 4940.
- (120) Di, Y.; Wang, X. C.; Thomas, A.; Antonietti, M. *ChemCatChem* **2010**, *2*, 834.
- (121) Li, Q. Y.; Yue, B.; Iwai, H.; Kako, T.; Ye, J. H. *J. Phys. Chem. C* **2010**, *114*, 4100.
- (122) Li, X. H.; Zhang, J. S.; Chen, X. F.; Fischer, A.; Thomas, A.; Antonietti, M.; Wang, X. C. *Chem. Mater.* **2011**, *23*, 4344–4348.
- (123) Takanabe, K.; Kamata, K.; Wang, X. C.; Antonietti, M.; Kubota, J.; Domen, K. *Phys. Chem. Chem. Phys.* **2010**, *12*, 13020.
- (124) Que, L.; Tolman, W. B. *Nature* **2008**, *455*, 333.
- (125) Sheldon, R. A.; Arends, I.; Ten Brink, G. J.; Dijkstra, A. A. *Acc. Chem. Res.* **2002**, *35*, 774.
- (126) Corma, A.; Garcia, H. *Chem. Soc. Rev.* **2008**, *37*, 2096.
- (127) Wang, Q.; Zhang, M. A.; Chen, C. C.; Ma, W. H.; Zhao, J. C. *Angew. Chem., Int. Ed.* **2010**, *49*, 7976.
- (128) Zhang, M. A.; Chen, C. C.; Ma, W. H.; Zhao, J. C. *Angew. Chem., Int. Ed.* **2008**, *47*, 9730.
- (129) Su, F. Z.; Mathew, S. C.; Lipner, G.; Fu, X. Z.; Antonietti, M.; Blechert, S.; Wang, X. C. *J. Am. Chem. Soc.* **2010**, *132*, 16299.
- (130) Chen, C. C.; Ma, W. H.; Zhao, J. C. *Chem. Soc. Rev.* **2011**, DOI: 10.1039/b92169h.
- (131) Yan, S. C.; Lv, S. B.; Li, Z. S.; Zou, Z. G. *Dalton Trans.* **2010**, 39, 1488.
- (132) Su, F. Z.; Mathew, S. C.; Lipner, G.; Fu, X. Z.; Antonietti, M.; Blechert, S.; Wang, X. C. *J. Am. Chem. Soc.* **2010**, *132*, 16299–16301.
- (133) Cui, Y. J.; Ding, Z. X.; Liu, P.; Antonietti, M.; Fu, X. Z.; Wang, X. C. *Phys. Chem. Chem. Phys.* **2012**, *14*, 1455–1462.
- (134) Zhang, J. S.; Zhang, G. G.; Chen, X. F.; Lin, S.; Moehlmann, L.; Dolega, G.; Lipner, G.; Antonietti, M.; Blechert, S.; Wang, X. C. *Angew. Chem., Int. Ed.* **2012**, *51*, 3183–3187.
- (135) Moehlmann, L.; Baar, M.; Rieß, J.; Antonietti, M.; Wang, X. C.; Blechert, S. *Adv. Synth. Catal.* **2012**, DOI: 10.1002/adsc.20110089.